Free Radical Biology and Medicine 89 (2015) 906–917

Contents lists available at ScienceDirect

Free Radical Biology and Medicine

journal homepage: www.elsevier.com/locate/freeradbiomed

Left ventricular diastolic dysfunction in Nrf2 knock out mice is associated with cardiac hypertrophy, decreased expression of SERCA2a, and preserved endothelial function

Ralf Erkens [a], Christian M. Kramer [a], Wiebke Lückstädt [a], Christina Panknin [a], Lisann Krause [a], Mathias Weidenbach [a], Jennifer Dirzka [a], Thomas Krenz [a], Evanthia Mergia [b], Tatsiana Suvorava [a], Malte Kelm [a], Miriam M. Cortese-Krott [a,*]

[a] Cardiovascular Research Laboratory, Division of Cardiology, Pneumology and Angiology, Medical Faculty, Heinrich Heine University of Düsseldorf, Düsseldorf, Germany
[b] Institute for Pharmacology and Toxicology, Ruhr-University Bochum, Bochum, Germany

ARTICLE INFO

Article history:
Received 24 September 2015
Accepted 9 October 2015
Available online 22 October 2015

Keywords:
Nrf2 KO
Echocardiography
eNOS
Translational research
Flow-mediated dilation
High-resolution ultrasound

ABSTRACT

Increased production of reactive oxygen species and failure of the antioxidant defense system are considered to play a central role in the pathogenesis of cardiovascular disease. The transcription factor nuclear factor (erythroid-derived 2)-like 2 (Nrf2) is a key master switch controlling the expression of antioxidant and protective enzymes, and was proposed to participate in protection of vascular and cardiac function. This study was undertaken to analyze cardiac and vascular phenotype of mice lacking Nrf2. We found that Nrf2 knock out (Nrf2 KO) mice have a left ventricular (LV) diastolic dysfunction, characterized by prolonged E wave deceleration time, relaxation time and total diastolic time, increased E/A ratio and myocardial performance index, as assessed by echocardiography. LV dysfunction in Nrf2 KO mice was associated with cardiac hypertrophy, and a downregulation of the sarcoplasmic reticulum Ca^{2+}-ATPase (SERCA2a) in the myocardium. Accordingly, cardiac relaxation was impaired, as demonstrated by decreased responses to β-adrenergic stimulation by isoproterenol ex vivo, and to the cardiac glycoside ouabain in vivo. Surprisingly, we found that vascular endothelial function and endothelial nitric oxide synthase (eNOS)-mediated vascular responses were fully preserved, blood pressure was decreased, and eNOS was upregulated in the aorta and the heart of Nrf2 KO mice. Taken together, these results show that LV dysfunction in Nrf2 KO mice is mainly associated with cardiac hypertrophy and downregulation of SERCA2a, and is independent from changes in coronary vascular function or systemic hemodynamics, which are preserved by a compensatory upregulation of eNOS. These data provide new insights into how Nrf2 expression/function impacts the cardiovascular system.

1. Introduction

The transcription factor nuclear factor (erythroid-derived 2)-like 2 (Nrf2) is a key master switch controlling the expression of antioxidant and protective enzymes [1–3]. An imbalance between pro-oxidants and anti-oxidant defense systems, defined as oxidative stress [4], has been linked to the development of atherosclerosis, as well as vascular and cardiac dysfunction and maladaptive cardiac remodeling [5]. Nrf2-target genes and their biochemical pathways regulate different physiological and pathophysiological processes including detoxification from xenobiotics and heavy metals [3], cancer [6], neurodegeneration [7], adipocyte differentiation [8], stroke [9], inflammation and related conditions, like metabolic disorders (e.g. diabetes) [10] and vascular aging [11]. Nrf2 knock out (KO) mice show a marked dysregulation of the biochemical pathways responsible for maintenance of redox state and defense mechanisms [3]. Therefore they could be considered as a model of chronic adaptation of the organism to oxidative stress [3]. From in vitro studies carried out in vascular cells and cardiomyocytes, it is clear that activation of Nrf2-dependent pathways exerts a protective effect against exogenous noxious stimuli, heavy metals and pro-oxidative damage [12–15]. In vivo activation of Nrf2 by pharmacological

Abbreviations: BP, blood pressure; CO, cardiac output; DP, developed pressure; DT, deceleration time; FMD, flow-mediated dilation; GC, guanylyl cyclase; IVRT, isovolumic relaxation time; KO, knock out; LV, left ventricular; MVET, mitral valve ejection time; Nrf2, nuclear factor (erythroid-derived 2)-like 2; PWV, pulse wave velocity; SV, stroke volume; SERCA2a, sarcoplasmic reticulum Ca^{2+}-ATPase; WT, wild type

* Correspondence to: Division of Cardiology, Pneumology and Angiology. Medical Faculty. Heinrich Heine University of Düsseldorf. Moorenstraße 5, 40225 Düsseldorf. Germany.
E-mail address: Miriam.Cortese@uni-duesseldorf.de (M.M. Cortese-Krott).

http://dx.doi.org/10.1016/j.freeradbiomed.2015.10.409

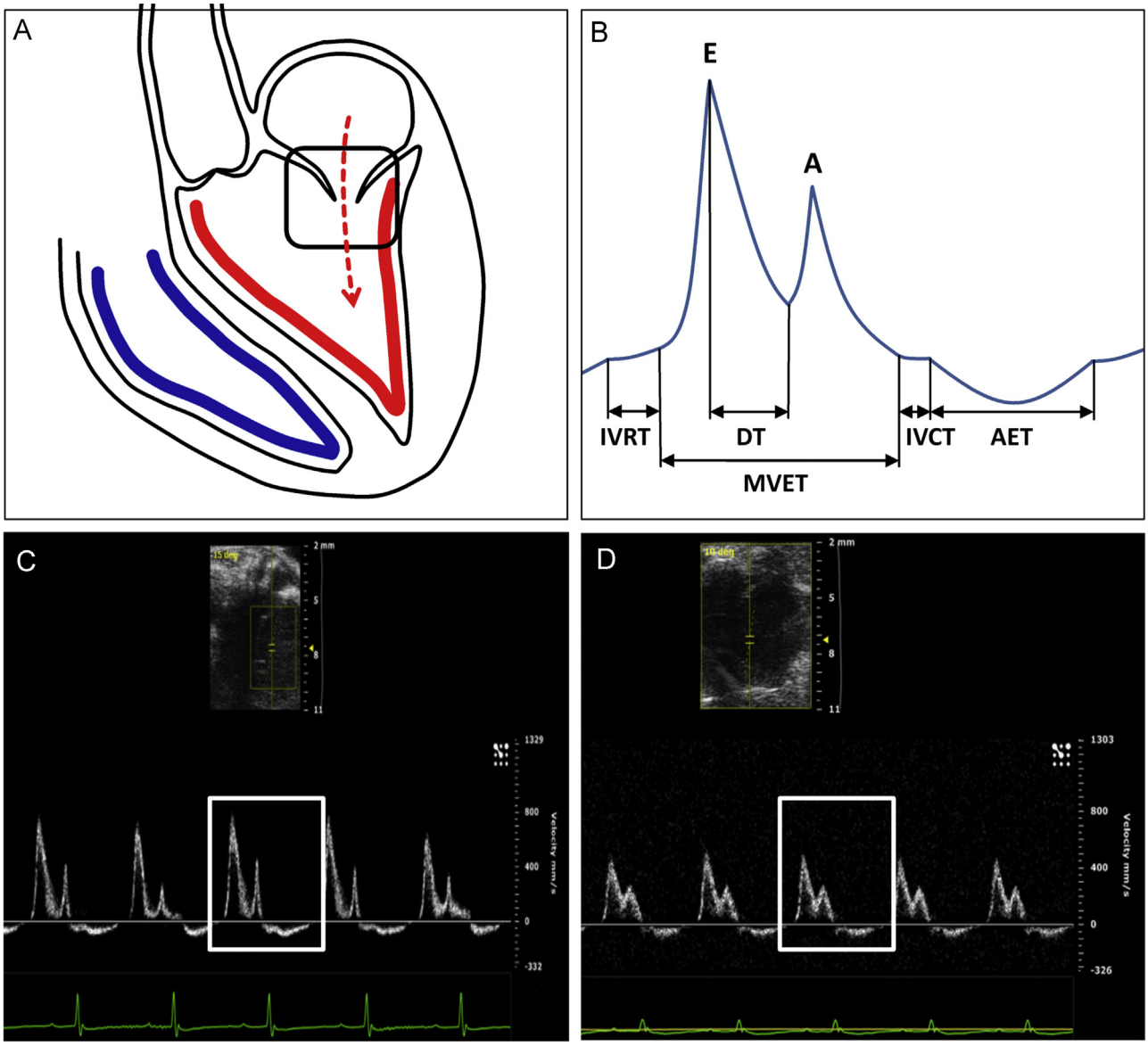

Fig. 1. Changes in mitral valve Doppler profile of Nrf2 KO mice. (A) Schematic representation of the mitral blood flow as seen in apical four-chamber view. The inset illustrates the detection window. **(B)** Analysis of mitral valve Doppler flow. The E peak (or wave) represents passive early diastolic filling, followed by the A wave, which is caused by atrial contraction. DT, deceleration time of the E wave; MVET, mitral valve ejection time (representing diastolic filling time); IVRT, isovolumic relaxation time; IVCT, isovolumic contraction time and AET, aortic ejection time (representing total systolic ejection time). **(C, D)** Representative images of a mitral valve Doppler profile in Nrf2 KO **(C)** and WT mice **(D)**.

stimuli (e.g. sulfide) [16], phytochemicals (e.g. sulforaphane), or other stimuli [17] protect the heart against ischemia/reperfusion injury, while lack of Nrf2 fully blocks these cardioprotective effects [16].

Considering the central role of Nrf2 in maintenance of tissue redox balance, we hypothesized that Nrf2-dependent biochemical pathways may play a role in preservation of cardiac and vascular function. In this study we aimed to investigate the cardiac and vascular phenotype, as well as systemic hemodynamics in Nrf2 KO mice as compared to WT littermates by using a multilevel translational approach. Cardiac and endothelial function of these mice were assessed non-invasively by high-resolution ultrasound, as done in clinical settings [18,19], and were compared to ex vivo analysis of cardiac contractility and coronary function in isolated perfused hearts. Specifically, left ventricular (LV) diastolic function was assessed by analyzing transmitral valve Doppler flow, while endothelial function was measured as flow-mediated dilation (FMD). We found that Nrf2 KO mice have an impaired LV diastolic function associated with LV hypertrophy and downregulation of sarcoplasmic reticulum Ca^{2+}-ATPase 2a (SERCA2a) in the myocardium. Consistently, we found an impaired myocardial relaxation, and disturbed responses to pharmacological modulators of Ca^{2+}homeostasis (isoproterenol/ouabain), while endothelial function was fully preserved via upregulation of endothelial nitric oxide synthase (eNOS). These data provide new insights into how Nrf2 expression/function impact the cardiovascular system.

2. Materials and Methods

2.1. Materials

Unless otherwise specified, chemicals were purchased from Sigma-Aldrich Co. LLC. (Deisenhofen, Germany). Materials for western blotting were purchased from Life technologies (Invitrogen, Darmstadt, Germany).

2.2. Animals

All experiments were approved by the LANUV according to the European Convention for the Protection of Vertebrate Animals used for Experimental and other Scientific Purposes (Council of Europe Treaty Series No. 123). Animal care was in accordance with the institutional guidelines. If not differently specified, male C57Bl/6 J mice were used as WT control (The Jackson Laboratory, Bar Harbor, ME, USA). Nrf2 KO/C57BL6J (BRC No. 01390) mice were obtained by Rinken (Koyadai, Tsukuba, Ibaraki, Japan) and crossed for more than 10 generations with C57BL/6 J. Moreover, eNOS KO mice with C57BL/6 J background were obtained from Dr. Axel Gödecke (Heinrich Heine University of Düsseldorf, Düsseldorf, Germany) [20]. For experiments, 5-6 month old male mice were used.

2.3. Cells

Pooled human umbilical vein endothelial cells (HUVECs) of a defined lot were obtained from Promocell (Heidelberg, Germany), cultured under standard conditions at 37 °C with 5% CO_2 in a commercial endothelial culture medium (Promocell) as previously described [21].

2.4. Measurement of reduced and total glutathione (GSH)

For determination of reduced and total GSH, aorta and heart of Nrf2 KO mice and WT mice were homogenized in ice cold 0.01 M HCl and sonicated for 30 s at 4 °C. After centrifugation at 14,000 × g for 10 minutes (min) at 4 °C, the supernatant was mixed with 5% sulfosalicylic acid (2.5% final concentration) to precipitate the proteins, and centrifuged again as described above. The clear supernatant was used for GSH measurements using the DetectX Fluorescent Detection Kit (Arbor Assays, Ann Arbor, MI, USA) following the manufacturer´s instructions. Oxidized glutathione (GSSG) was calculated as (total GSH-Free GSH)/2. Moreover, the ratio of reduced GSH/GSSG was calculated.

2.5. Assessment of cardiac function

Cardiac imaging was carried out by using a high-resolution ultrasound system (18-38 MHz; Vevo 2100, Visual Sonics Inc., Toronto, Canada), and the manufacturer's analysis software. LV volume, stroke volume (SV), cardiac output (CO) and ejection fraction (EF) were calculated in B-mode by identification of maximal and minimal cross-sectional area. Additionally, LV systolic function was determined as fractional shortening (FS) in the longitudinal axis. LV diastolic function was measured by analyzing the characteristic flow profile of the mitral valve Doppler and tissue Doppler flow (Fig. 1B), which was visualized in apical four-chamber view. The E deceleration time (DT) was taken from the maximum of the E wave to its baseline. Mitral valve ejection time (MVET) represents total diastolic time (duration of diastolic filling of the left ventricle) and was analyzed by calculating velocity time integral of E and A wave. Isovolumic relaxation time (IVRT) was determined as the interval between aortic valve closure and mitral valve opening; isovolumic contraction time (IVCT) represents the interval between mitral valve closure and aortic valve opening. The myocardial performance index (MPI or Tei-index) [22], which is an objective parameter incorporating systolic and diastolic time intervals and defines global systolic and diastolic ventricular function, was calculated as the sum of IVRT and IVCT divided by aortic ejection time (= mitral valve no flow time) [23]. LV mass was calculated as ((1.053*((LVEDD+LVPW,ED+IVS,ED)3-LVEDD3))*0.8) and further normalized for body weight. Cardiac mass was also calculated from the ratio between heart weight and body weight (Table 2).

2.6. Assessment of vascular function and stiffness in vivo

Vascular function was assessed with a Vevo 2100 with a 30–70 MHz linear array microscan transducer (Visual Sonics). The method consists in the analysis of changes in vessel diameter in response to shear stress after vascular occlusion by using a cuff; this method was developed from a procedure published previously [24] with substantial modifications, which allowed us to measure changes in vessel diameter both during occlusion and after cuff-release. During the experiment, mice were kept under 1.5-2% isoflurane anesthesia, a heart rate of 400–500 bpm, a breathing rate of about 100 breaths per minute, and a 37 °C body temperature. The transducer was placed using a stereotactic holder and was adjusted manually to visualize the arteria iliaca externa as depicted in supplementary information (SI Fig. S1). The vessel was identified by its characteristic blood flow pattern by the duplex ultrasound method. A vascular occluder (8 mm diameter, Harvard Apparatus, Harvard, Boston, MA, USA) was placed around the lower limb. For measurements of vascular function, first baseline images of the vessel were recorded, afterwards the occluder (positioned above the knee) was inflated to 200 mmHg, and pressure was kept constant for 5 min (Druckkalibriergerät KAL 84, Halstrup Walcher, Kirchzarten, Germany) to occlude the vessels; then the occluder was deflated to induce shear stress and flow-mediated dilation (FMD). The diameter of the vessel was determined at the indicated time points (see main text) both during cuff inflation and after cuff release, proximal to the cuff. Changes in vessel diameter were calculated as percent ratio (%) = [diameter (max) / diameter (baseline)] x 100. Baseline values for WT were 0.27 ± 0.06 mm (n = 12) and for Nrf2 KO 0.29 ± 0.04 mm (n = 14). The maximal percent changes in dilation as compared to baseline were calculated as Δ% = [diameter (max) – diameter (baseline) / diameter (baseline)] × 100. Where indicated, the same measurements were performed in the presence of the specific nitric oxide synthase (NOS) inhibitor 2-ethyl-2-thiopseudourea hydrobromide (ETU) infused intraperitoneally (i.p. 1.3 μmol/kg/min) for 30 min before determination of vascular function. In these experiments baseline measurements were determined both before and after administration of ETU (WT+ETU 0.21 ± 0.03 mm vs. WT untreated 0.27 ± 0.05 mm, n = 5; Nrf2 KO+ETU 0.27 ± 0.03 mm vs. Nrf2 KO untreated 0.28 ± 0.05 mm, n = 6).

Vascular stiffness was assessed as pulse wave velocity (PWV) in the arteria carotis communis as described previously [25] with some modifications. B-mode images were obtained by placing the transducer above the arteria carotis to obtain longitudinal images of this vessel. Images were acquired proximal and distal to the carotis bifurcation in M-mode and PW-Doppler, and the distance between these points was determined (SI Fig. S2). PWV was calculated as a ratio between distance/time interval, determined by measuring the interval time from the R wave (recorded with the electrocardiogram) to either systolic notch in M-mode, or alternatively to the peak of systolic component in PW Doppler.

2.7. Assessment of vascular function in aortic rings ex vivo

Thoracic aortas were explanted and analyzed in an organ bath as previously described [26]. Experiments started after an equilibration phase of 60 min. Endothelial function was assessed by administration of cumulative doses of acetylcholine (ACh; 0.1 nM–10 μM). After washing, vascular contractility was determined by applying cumulative doses of the α_1-adrenergic receptor agonist phenylephrine (PHE; 0.1 nM – 10 μM). Subsequently, NO-dependent vasodilation was induced by applying a cumulative dose of sodium nitroprusside (SNP; 0.01 pM–10 μM). The half-maximal

effective concentration (EC_{50}) of PHE and ACh were determined in preliminary experiments.

2.8. Assessment of cardiac function in isolated perfused hearts

Mice were anesthetized by i.p. injection of 100 mg/kg ketamine (Ketanest®) and 10 mg/kg xylazine (Rompun®), and anticoagulated with heparin (250 IU i.p.). The heart was explanted and retrograde perfused at 100 mmHg with a modified Krebs-Henseleit buffer containing NaCl (118 mM), KCl (4.7 mM), $MgSO_4$ (0.8 mM), $NaHCO_3$ (25 mM), KH_2PO_4 (1.2 mM), glucose (5 mM), pyruvic acid (1.9 mM) and $CaCl_2$ (2.5 mM) gassed with carbogen gas, as previously described [27]. Left ventricular pressure (LVP), perfusion pressure, aortic flow, and heart rate were measured continuously by using an analog–digital converter (2,000 Hz) and dedicated software (EMKA Technologies, Paris, France). Experiments started after an equilibration phase of about 20 min. To assess coronary endothelial function we induced 20 seconds (s) of ischemia followed by 5 min of reperfusion. Bradykinin (5 μmol/ml), adenosine (1 μmol/ml) and isoproterenol (12 pmol/ml) were infused into the aortic cannula one after another with 10-15 min washout intervals in between.

2.9. Assessment of natriuretic peptides, β-MHC, and TNFα in serum

Mice were anesthetized as described above, and blood was taken from cardiac punction and transferred directly into serum collection tubes. After 20 min of incubation at room temperature, tubes were centrifuged at 2,500 × g for 3 min, and serum was frozen and kept at -20 °C until analysis. Atrial natriuretic peptide (ANP), NTproBNP, β-MHC and TNFα were analyzed using high sensitive ELISA Kits purchased from Hölzel-Biotech (Köln, Germany) and carried out as by manufacturer's instructions.

2.10. Assessment of systemic hemodynamics

Invasive assessment of hemodynamic parameters was carried out by using a 1.4 F Millar pressure-conductance catheter (SPR-839, Millar Instrument, Houston, TX, USA) placed into the left ventricle through the right carotid artery according to the closed chest method as described [28]. Pressure was recorded by a Millar Box and analyzed with LabChart 7 (AD Instruments, Oxford, UK) to assess LV developed pressure, rate of pressure development (dP/dt_{max}) and rate of pressure decrease (dP/dt_{min}). The effects of the cardioglycoside ouabain (i.p. 1 nmol/kg) on these parameters, as well as the effects of NOS inhibition by ETU on systolic and diastolic pressure (i.p. 1.3 μmol/kg/min as already described) were also determined.

2.11. Organ explantation for biochemical parameters

Mice were anesthetized as described above. Organs were explanted after systemic perfusion with cold phosphate buffered solution pH 7.4 and immediately frozen in liquid nitrogen.

2.12. Determination of eNOS-dependent guanylyl cyclase activation

The eNOS-dependent activation of guanylyl cyclase (GC) in response to carbachol and the resulting increase in intracellular cGMP concentration was measured by radioimmunoassay (RIA) as described before [29], with minor modifications. Explanted aortas were prepared in Krebs-Henseleit buffer bubbled with carbogen gas and cutted in rings. The rings were incubated at 37 °C for 10 min, and treated for 3 min with carbachol (30 μM) to stimulate eNOS-dependent activation of the NO-dependent GC and cGMP synthesis. Immediately thereafter, aorta fragments were frozen in liquid nitrogen. Frozen samples were homogenized and lysed in 70% ethanol. After centrifugation (14,000 × g, 15 min, 4 °C), the supernatants were dried in a Speed-Vac (Thermoscientific, Braunschweig, Germany) and used for measurement of cGMP. Dried pellets were lyzed in a solution of 0.1% SDS in 0.1 M NaOH and protein concentration was assessed by Lowry assay (DC Protein Assay, Bio-Rad).

2.13. Western blot analysis

Organs were weighted, lysed in RIPA buffer (1% NP40, 0.5% sodium deoxycholate, 0.1% SDS in PBS) containing a cocktail of protease and phosphatase inhibitors (Pierce) and homogenized at 4 °C by using TissuRuptor (Qiagen, Hilden, Germany) and frozen at −20 °C. Lysates were sonicated for 3 min at 4 °C and centrifuged at 4,000 × g for 10 min at 4 °C. Total protein concentration of the supernatant was determined by Lowry assay. Samples (80 μg heart lysate; 20 μg aorta lysate) and HUVECs (positive control, 5 μg) were loaded in 7% or 3–8% NuPAGE Tris-Acetate pre-cast gels (Invitrogen) following the manufacturer's instructions. After transfer onto PVDF membrane Hybond P (Amersham Biosciences, Munich, Germany), proteins were stained with Ponceau S (SERVA Electrophoresis GmbH, Heidelberg, Germany). The membranes were blocked for 2 hours with 5% BSA (Bio-Rad) in T-TBS (10 mM Tris, 100 mM NaCl, 0.1% Tween) and incubated overnight at 4 °C with a mouse anti-eNOS (1 : 250, custom made from #624086 anti eNOS/NOS type III antibody, stock: 1 mg/ml in PBS pH 7.4, BD Bioscience, Erembodegem, Belgium), a rabbit anti-phospho-eNOS (Ser1177) (1 : 500; #9571, Cell Signaling, Cambridge, UK), or monoclonal mouse anti-α-Tubulin (1 : 5,000, #T6199, Sigma-Aldrich) in T-TBS. After washing for 1 hour in T-TBS, the membranes were incubated with HRP-conjugated goat anti-mouse or anti-rabbit antiserum (1 : 5,000; BD Biosciences). The bands were visualized by autoradiography on Hyperfilm ECL (Amersham Biosciences) using SuperSignal West Pico Chemiluminescent Substrate (Pierce) or SuperSignal West Femto Chemiluminescent Substrate (Pierce). Band intensity quantification was carried out using ImageJ. Further determination of SERCA2a and eNOS/phospho-eNOS (Ser1177) in heart and aortic tissue as well as GC1α in the aorta were carried out essentially as described above with following modifications: for detection of SERCA2a and NO-GC1α we used a nitrocellulose membrane, and for blocking and detection we used Amersham ECL Prime blocking agent and Amersham ECL Select Western Blotting Detection Reagent in an Image Quant (GE Healthcare, Freiburg, Germany). We used following antibodies: a rabbit polyclonal anti-SERCA2a (1 : 4,000, #0814-01, Badrilla Ltd., Leeds, UK), rabbit polyclonal anti-GC1α (1 : 1,000, #G4280, Sigma-Aldrich), mouse monoclonal anti-GAPDH (1 : 4,000, #G8795, Sigma-Aldrich) and rabbit polyclonal anti-actin (1 : 5,000, #A2066, Sigma-Aldrich).

2.14. Measurement of nitrite and nitrate in mouse plasma

Blood samples were collected by intra-cardiac puncture and transferred to heparinized tubes. The resulting plasma was analyzed by HPLC as described previously in detail [30].

2.15. Statistical analysis

If not differently specified, the results are given as mean ± standard error of the mean (SEM). For repeated measurements, data were analyzed by 1-way or 2-way ANOVA as appropriate followed by Bonferroni's or Sidak's post hoc tests. Where indicated, unpaired Student's t-test was used to determine if two groups of data were significantly different. Normal distribution was tested by D'Agostino-Pearson test Comparisons with $p < 0.05$

was considered as statistical significant.

3. Results

3.1. Redox imbalance in the heart and vessels of Nrf2 KO mice

To determine whether lack of Nrf2 affects the antioxidant capacity of the myocardium and vascular tissues, we first evaluated the levels of total glutathione (GSH) and reduced "free" (GSH) in the tissues of Nrf2 KO mice (Table 1). In aorta we found decreased total GSH levels, increased GSSG levels, and decreased GSH/GSSG ratio, as compared to WT mice. In the heart of Nrf2 KO mice, although the levels of total GSH were decreased, we found a compensatory increase in the GSH/GSSG ratio. These results show that Nrf2 KO mice have decreased GSH-dependent antioxidant and detoxification capacity. These findings are in line with previous data showing downregulation of phase II antioxidant enzymes, including enzymes responsible for the de novo synthesis of GSH in Nrf2 KO mice [16,31,32].

3.2. Diastolic dysfunction, cardiac hypertrophy and downregulation of SERCA2a in Nrf2 KO mice in vivo

To analyze the functional consequences of redox dysregulation in the heart of Nrf2 KO mice, we carried out a non-invasive assessment of cardiac function by high-resolution ultrasound. In Nrf2 KO mice systolic function is fully preserved, as indicated by ejection fraction and fractional shortening, which were not significantly different as compared to WT littermates (Table 2). Accordingly, cardiac output (CO) and stroke volume (SV) were also not significantly different in Nrf2 KO as compared to WT mice (Table 2). To measure LV diastolic function, we visualized the mitral inflow by pulse wave Doppler imaging in apical four chamber view (schematically depicted in Fig. 1A), and analyzed the Doppler flow profile by quantifying the characteristic waves (Fig. 1B). Fig. 1C and D show representative pictures of the mitral flow Doppler profile: the E peak (or wave) represents passive early diastolic filling, followed by the A wave, which is caused by atrial contraction. The overall profile of the flow Doppler waves of Nrf2 KO mice (Fig. 1C) was largely different as compared to WT littermates (Fig. 1D). We found a significantly prolonged DT in Nrf2 KO mice as compared to WT littermates (Fig. 2A), pointing to an impaired LV relaxation. Diastolic dysfunction in Nrf2 KO mice was confirmed by 1.5-fold prolonged MVET and IVRT as compared to WT littermates, whereas contraction time was not different (Table 2). Moreover, the E/A ratio and the E/E´ ratio was 68% increased in Nrf2 KO mice as compared to WT littermates (Fig. 2A, Table 2).

Table 1
Decreased levels of GSH in the heart and in the aorta of Nrf2 KO mice. Data are reported as mean ± SD. n = number of mice; differences between the two groups were calculated by unpaired t-test after testing for normal distribution and equal variances. $p < 0.05$ was considered as significant and marked in bold.

Parameter	Unit	WT	Nrf2 KO	p (WT vs. Nrf2 KO)
Heart	n	7	7	
Total GSH	nmol/mg protein	16.6 ± 0.4	13.4 ± 0.2	**< 0.0001**
Free GSH	nmol/mg protein	14.5 ± 0.4	12.1 ± 0.3	**0.0005**
GSSG	nmol/mg protein	1.1 ± 0.1	0.6 ± 0.1	**< 0.0001**
GSH/GSSG		13.4 ± 0.8	19.7 ± 1.9	**0.0102**
Aorta	n	7	5	
Total GSH	nmol/mg protein	16.9 ± 0.8	12.9 ± 0.9	**0.0086**
Free GSH	nmol/mg protein	16.7 ± 0.8	12.1 ± 0.8	**0.0034**
GSSG	nmol/mg protein	0.1 ± 0.1	0.4 ± 0.1	**0.0331**

Table 2
Echocardiographic parameters assessed in vivo by high-resolution ultrasound. Data are reported as mean ± SD; n = number of mice. Differences between the two groups were calculated by unpaired t-test after testing for normal distribution and equal variances; $p < 0.05$ was considered as significant and marked in bold.

Parameter	Unit n	WT 10	Nrf2 KO 12	p (WT vs. Nrf2 KO)
Weight				
Body weight	g	35 ± 3	33 ± 3	0.27
Heart weight	mg	200 ± 18	214 ± 25	0.25
Parameters of cardiac function and mass				
Heart Rate	BPM	393 ± 21	372 ± 23	0.056
Cardiac Output	ml/min	13.1 ± 2.7	13.0 ± 2.6	0.97
Stroke Volume	µl	30.6 ± 5.3	35.8 ± 6.8	0.09
Ejection Fraction	%	50.1 ± 9.3	41.4 ± 7.7	0.08
Fractional Shortening	%	10.2 ± 3.2	10.8 ± 4.4	0.72
LV Mass corrected	mg	69.7 ± 15.2	88.6 ± 17.1	0.054
Endsystolic Volume	µl	32.8 ± 9.8	54.5 ± 17.2	**0.005**
Enddiastolic Volume	µl	63.6 ± 10.1	90.3 ± 20.8	**0.003**
Myocardial Performance Index		0.4 ± 0.1	0.8 ± 0.2	**0.0005**
LV Mass/Body Weight Ratio		2.0 ± 0.3	2.7 ± 0.5	**0.013**
Heart Weight/Body Weight Ratio		5.5 ± 0.3	6.6 ± 1.0	**0.029**
Mitral flow doppler				
E/A		1.5 ± 0.3	2.2 ± 0.6	**0.0158**
E/E'		20.9 ± 4.3	30.8 ± 6.7	**0.0094**
Deceleration Time	ms	13.1 ± 4.4	30.0 ± 4.5	**< 0.0001**
Diastolic Time (MVET)	ms	58.5 ± 8.9	76.9 ± 15.5	**< 0.0001**
Isovolumic Relaxation Time	ms	17.8 ± 2.6	23.6 ± 4.4	**0.0046**
Isovolumic Contraction Time	ms	10.2 ± 4.1	9.9 ± 3.6	0.89

These results indicate an impaired diastolic filling of the left ventricle. Importantly, MPI, which is considered as an objective parameter of LV function, was also significantly increased in Nrf2 KO mice (Fig. 2A), indicating a reduced myocardial relaxation in Nrf2 KO mice. Heart rate in Nrf2 KO mice was not different as compared to WT littermates (Table 2).

Diastolic dysfunction in Nrf2 KO mice was associated with LV hypertrophy, as determined by the significant increase of both the LV mass to body weight ratio, and heart weight to body weight ratio (Fig. 2A, Table 2). Cardiac hypertrophy was not accompanied by an increase in circulating natriuretic peptides, as serum levels of N-terminal of the prohormone brain natriuretic peptide (NT-proBNP), and atrial natriuretic peptide (ANP) were not different as compared to WT mice; nor it was related to a pro-inflammatory state, as the number of inflammatory cells and levels of circulating TNFα were not increased in Nrf2 KO mice (SI Tab.S3). In addition, we found a significant decrease in the expression of the SERCA2a in the myocardium of Nrf2 KO mice as compared to WT mice (Fig. 2B).

Taken together, Nrf2 KO mice show an impaired LV diastolic function, correlated to cardiac hypertrophy and downregulation of SERCA2a.

3.3. Decreased myocardial relaxation and impaired Ca^{2+} homeostasis in the heart of Nrf2 KO mice

Next, we aimed to evaluate whether changes in SERCA2a expression led to decrease in myocardial relaxation and impaired Ca^{2+} homeostasis. We analyzed the effects of β-mimetic stimulation by isoproterenol on cardiac function in a Langendorff system (Fig. 3A). We found a significant reduced response to the application of isoproterenol in Nrf2 KO hearts as compared to WT littermates, measured by a decrease in developed pressure (DP)

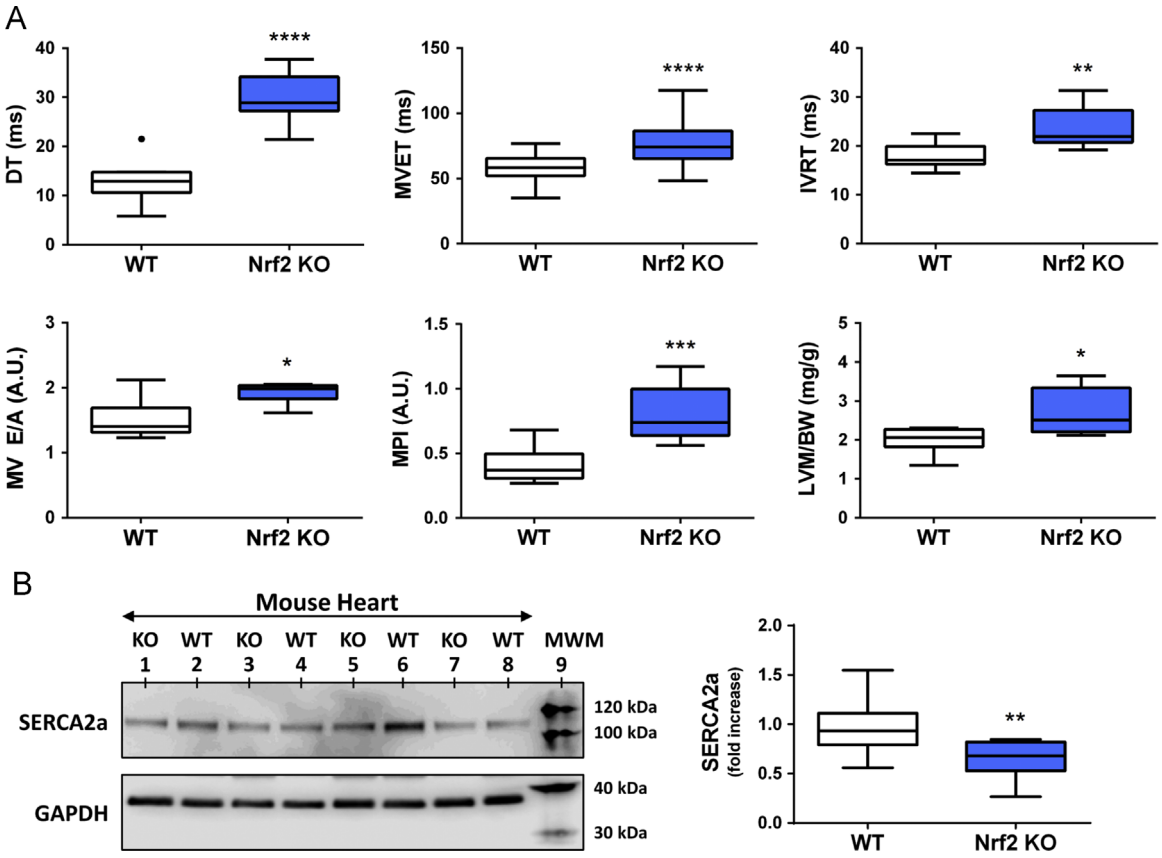

Fig. 2. LV-diastolic dysfunction, cardiac hypertrophy and decreased expression of SERCA2a in Nrf2 KO mice. (A) Nrf2 KO mice show impaired myocardial relaxation with prolonged deceleration time (DT), mitral valve ejection time (MVET), increased relaxation time (IVRT), E to A ratio, and myocardial performance index (MPI) as compared to WT mice. Nrf2 KO mice present cardiac hypertrophy as determined by increased LV-mass to body weight ratio. Parameters were assessed by echocardiography (WT: n = 10, Nrf2 KO: n = 12); unpaired t-test * $p < 0.05$; ** $p < 0.01$; **** $p < 0.0001$. **(B)** SERCA2a expression in the myocardium of Nrf2 KO was decreased as compared to WT mice (SERCA2a is shown in the upper panel and GAPDH was used as loading control; MWM, molecular weight marker. KO = Nrf2 KO mice). Left panel: representative of 3 independent blots. Right panel: densitometric quantification (WT: n = 8, Nrf2 KO: n = 8); unpaired t-test; ** $p < 0.01$.

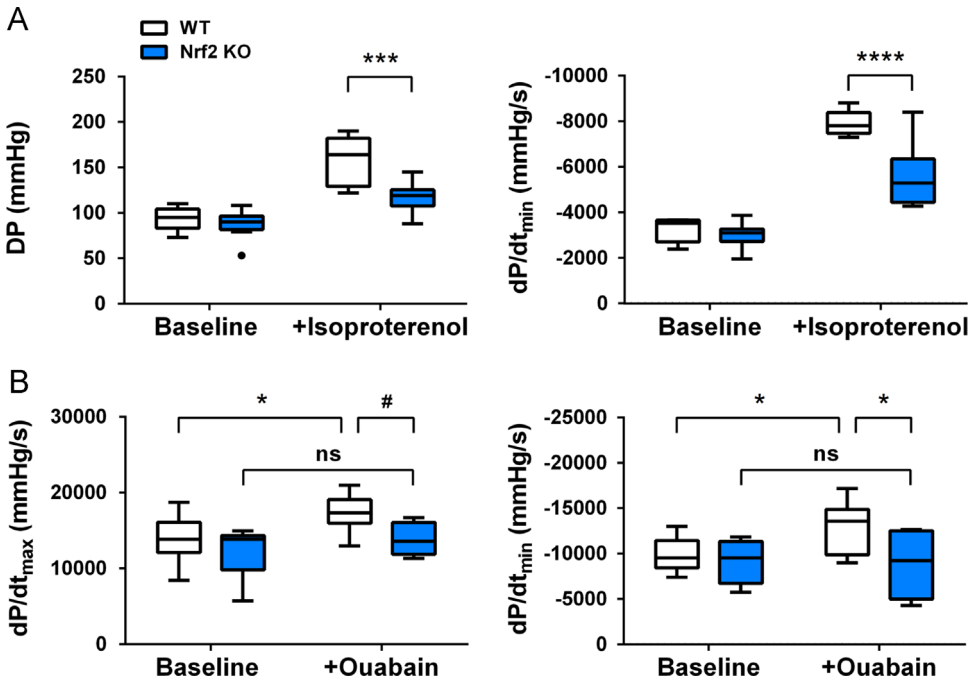

Fig. 3. Impaired cardiac relaxation in response to isoproterenol (ex vivo) and ouabain (in vivo) in Nrf2 KO hearts. (A) Developed pressure and dP/dt_{min} before and after injection of 12 nM isoproterenol in isolated perfused hearts (WT: n = 8, KO: n = 9); 2-way-ANOVA WT vs. KO $p < 0.001$ for both panels. **(B)** Ouabain (1 nmol/kg i.p.) increased dP/dt_{max} and dP/dt_{min} in WT mice, but not in Nrf2 KO mice as assessed by Millar catheter (WT: n = 7, KO: n = 7). 2-way ANOVA WT vs. Nrf2 KO $p < 0.01$ for both panels, Sidak's * $p < 0.05$, *** $p < 0.001$, **** $p < 0.0001$; unpaired t-test # $p < 0.05$.

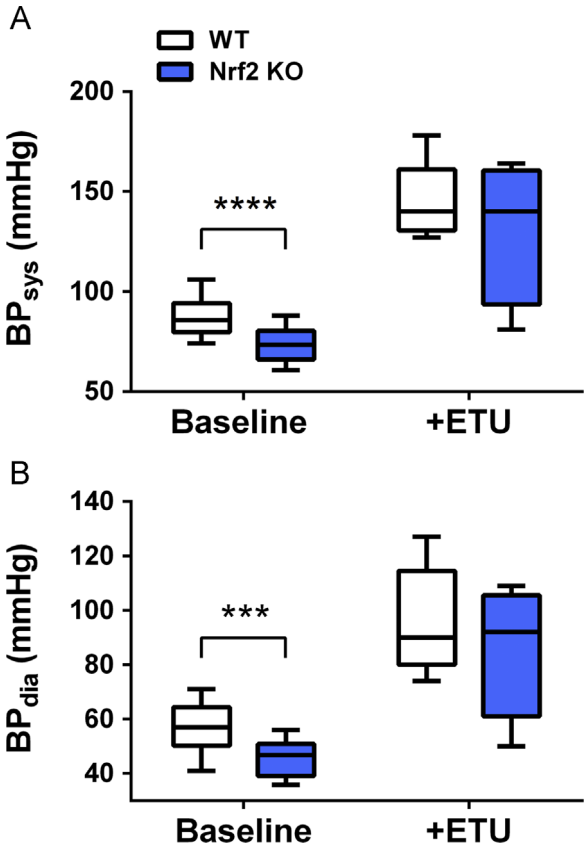

Fig. 4. Decreased systolic and diastolic blood pressure in Nrf2 KO mice. (A) Systolic and **(B)** diastolic blood pressure were significantly decreased in Nrf2 KO mice as compared to their littermates, as assessed invasively by Millar catheter in anesthetized mice. Application of ETU results in a significant increase in systolic and diastolic pressure both in WT and Nrf2 KO mice (WT: n = 12; KO: n = 12). Unpaired t-test *** $p < 0.001$; **** $p < 0.0001$.

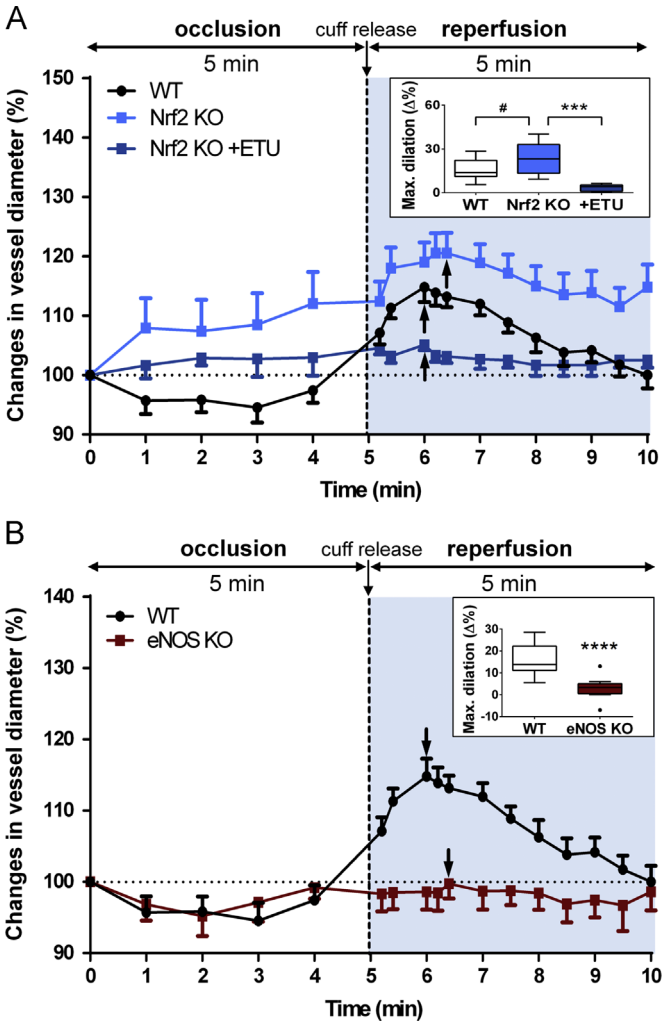

Fig. 5. Fully preserved NOS-dependent endothelial function in Nrf2 KO mice. (A) Changes in vessel diameter (% ratio vs. baseline diameter) during occlusion (white panel) and after releasing the cuff in WT mice (black line), in untreated Nrf2 KO mice (blue line), or during continuous infusion of the NOS inhibitor ETU (dark blue line). The black arrow represents the time point of maximal dilation. Inset: box plot according to Tukey representing the max percent change in dilation. (WT: n = 12; Nrf2 KO: n = 14; Nrf2 KO+ETU: n = 6; 1-way ANOVA $p < 0.001$, Bonferroni's *** $p < 0.001$; unpaired t-test # $p < 0.05$). **(B)** Changes in vessel diameter (% ratio vs. baseline diameter) in eNOS KO mice vs. WT mice. (WT: n = 12; eNOS KO: n = 13; unpaired t-test **** $p < 0.0001$).

(Fig. 3A, left panel) and dP/dt_{min} (Fig. 3A, right panel), while dP/dt_{max} was not different (SI Tab. S1). Adenosine and bradykinin application increased coronary flow in Nrf2 KO to the same extent as they did in WT hearts (SI Tab. S1). Intraperitoneal administration of the cardiac glycoside ouabain increased significantly dP/dt_{max} and dP/dt_{min} in WT mice as compared to untreated WT mice. Instead, the same dose of ouabain did not cause any significant response in Nrf2 KO mice as compared to untreated Nrf2 KO mice (Fig. 3B; SI Tab. S2).

Taken together, the reduced response of Nrf2 KO hearts to isoproterenol ex vivo (Fig. 3A) and ouabain in vivo (Fig. 3B) demonstrate that Nrf2 KO mice show a significantly impaired cardiac response to pharmacological regulation of cytosolic Ca^{2+} homeostasis as compared to WT littermates.

3.4. *Decreased blood pressure, preserved endothelial function and eNOS upregulation in the vessels and in the heart of Nrf2 KO mice*

Diastolic dysfunction is commonly associated with hypertension state and/or changes of the total peripheral resistance. Blood pressure was assessed invasively by using a pressure-conductance-catheter (Millar catheter) inserted in the ascending aorta of Nrf2 KO mice and WT littermates (Fig. 4 A, B). We found that systolic and diastolic blood pressure were significantly decreased in Nrf2 KO mice as compared to WT littermates. Application of NOS inhibitor ETU resulted in a significant increase in blood pressure both in WT- and Nrf2 KO mice.

Vascular endothelial function in Nrf2 KO mice were measured respectively in vivo (Fig. 5 and SI Fig. S4) as well as ex vivo in aortic rings (SI Fig. S5), while coronary vascular function was measured in isolated perfused hearts (SI Tab. S1). We found that maximal dilation of the arteria iliaca externa after 5 min of vascular occlusion was significantly increased in Nrf2 KO mice as compared to WT mice (Fig. 5A), indicating a fully preserved vascular function in this mice. This response was completely blocked by administration of the specific NOS-inhibitor ETU (Fig. 5A). Accordingly, eNOS KO mice showed no dilatory response to shear stress after occlusion as compared to WT mice (Fig. 5B), confirming that the FMD response mainly depends on eNOS-dependent vasodilatory pathways. Data demonstrating a fully preserved FMD response are consistent with ex vivo data showing preserved relaxation of aortic rings in Nrf2 KO mice (SI Fig. S5), and preserved coronary endothelial function in Nrf2 KO isolated perfused hearts (SI Tab. S1). In Nrf2 KO aortic rings we observed a rightward shift of the PHE dose-response contractility curve, indicating an impaired contractile response of Nrf2 KO aortic rings to α-adrenergic stimulation (SI Fig. S5B). As previously observed in human vessels [19], vascular occlusion induced vasoconstriction in WT (Fig. 5A, white panel) and eNOS KO

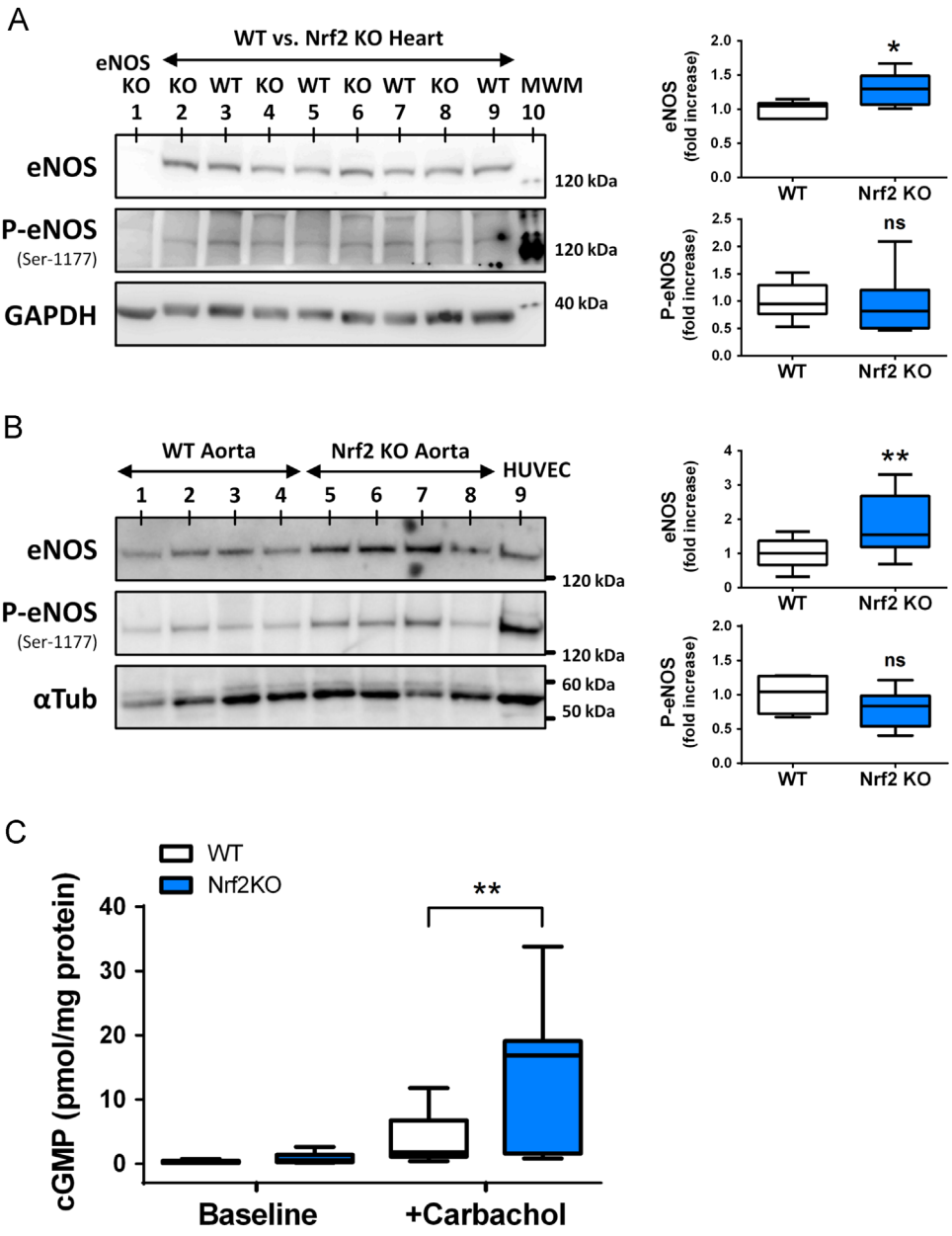

Fig. 6. Increases in eNOS expression in the heart and aorta, and eNOS-dependent stimulation of cGMP synthesis in aortic rings of Nrf2 KO mice. (A) Representative western blot showing increases in eNOS expression in the heart of Nrf2 KO mice; unpaired t-test * $p < 0.05$; ** $p < 0.01$; MWM, molecular weight marker. HUVECs, human umbilical endothelial cells (positive control). Right panel: densitometric quantification of eNOS levels (vs. loading control) and phosphorylation levels (P-eNOS vs. total eNOS); (WT: $n = 7$; Nrf2 KO: $n = 7$). **(B)** Representative western blot showing increases in eNOS expression in the the aorta of Nrf2 KO mice (WT: $n = 15$; Nrf2 KO: $n = 14$). Right panel: densitometric quantification of western blots; unpaired t-test * $p < 0.05$; ** $p < 0.01$. **(C)** Increased cGMP production in response to carbachol-mediated stimulation of eNOS in Nrf2 KO aortic rings as compared to WT controls (2-5 aortic rings/mouse; WT: $n = 3$; Nrf2 KO: $n = 3$). 1-way ANOVA $p < 0.0001$, Tukey's ** $p < 0.001$.

mice (Fig. 5B, white panel) [19]. Instead, Nrf2 KO mice show a significant vasodilatory response during occlusion (Fig. 5A, white panel).

Vascular stiffness in Nrf2 KO mice was not different as compared to WT mice, as evidenced by no changes in pulse wave velocity (PWV) measured in the arteria carotis communis (WT: 0.91 ± 0.21 m/s, Nrf2 KO: 0.93 ± 0.30 m/s; $n = 10$). In eNOS KO mice PWV was significantly increased as compared to WT mice (PWV WT: 0.99 ± 0.21 m/s, eNOS KO: 1.66 ± 0.83 m/s; $n = 6$; t-test $p = 0.0238$).

Consistent to a fully preserved endothelial function, eNOS expression was significantly up-regulated in the heart (Fig. 6A) and in the aorta (Fig. 6B) of Nrf2 KO mice as compared to WT littermates. Myocardial and aortic eNOS phosphorylation levels at Ser1177 were not changed (Fig. 6 A, B). To test for functionality of eNOS in the vascular wall, we stimulated the eNOS-dependent cGMP synthesis in aortic explants by treatment with carbachol, as done before [29]. Interestingly, Nrf2 KO mice showed higher carbachol-induced cGMP production as compared to WT mice, confirming that eNOS is functional in the aorta of Nrf2 KO mice (Fig. 6C). The basal cGMP levels in aorta (Fig. 6C) and heart (SI Fig. S3B) and the circulating nitrite/nitrate levels (SI Fig. S3A) were not different as compared to the WT controls.

To summarize, these results demonstrate that Nrf2 KO mice have a decreased blood pressure, a preserved endothelial function and an eNOS upregulation in the vessels and in the heart.

4. Discussion

This study was undertaken to analyze cardiac and vascular

phenotype of mice lacking the transcription factor Nrf2. We found that Nrf2 KO mice have a LV diastolic dysfunction, cardiac hypertrophy and impaired Ca^{2+} homeostasis in the myocardium, while vascular function is fully preserved via compensatory upregulation of eNOS. Specifically, Nrf2 KO mice show 1) preserved systolic function, but a significantly impaired LV diastolic function, with prolonged E wave, DT, MVET, IVRT, total diastolic time, increased E/A ratio and increased MPI, as assessed by echocardiography; 2) LV hypertrophy; 3) downregulation of SERCA2a in the myocardium; 4) an impaired cardiac relaxation, as demonstrated by an increase in IVRT, and a decreased cardiac response to isoproterenol ex vivo, and to ouabain in vivo; 5) hypotension, associated with a fully preserved endothelial function in conduit and coronary vessels; and 6) increased eNOS expression in the aorta and in the heart. These results clearly show that LV dysfunction in Nrf2 KO mice is independent from changes in the coronary vascular function or systemic hemodynamics, and rather caused by cardiac hypertrophy and downregulation of SERCA2a. These data provide new insights into how Nrf2 expression/function impacts the cardiovascular system.

4.1. Diastolic dysfunction, cardiac hypertrophy and dysregulation of Ca^{2+} homeostasis in Nrf2 KO mice

There is compelling evidence demonstrating that Nrf2-dependent transcriptional regulation of antioxidant and detoxifying enzymes play a fundamental protective role in almost any cell and tissue of the body [11,33], including the heart and the vessels [8,12,16,31,32,34–37]. In vitro and in vivo studies have shown that pharmacological activation of Nrf2 protects cardiomyocytes against increased oxidative and hemodynamic stress, while lack of Nrf2 blocks these effects [16,32]. An increased production of radical oxygen species, a decreased availability of reduced glutathione, and decreased expression/activity of protective enzymes (including glutathione peroxidase, catalase, superoxide dismutase) have been proposed to participate to the pathogenesis of cardiomyopathies and heart failure [38,39]. However, a direct molecular link between redox imbalance, oxidative stress and the molecular mechanisms leading to cardiac dysfunction and heart failure is difficult to be defined in detail, also because just few animal models of oxidative stress-mediated cardiac dysfunction exist.

Nrf2 KO mice can be considered as a model of chronic adaptation to oxidative stress, which may allow studying the functional consequences of a chronic redox imbalance on cardiac and vascular function. By carrying out a comprehensive echocardiographic evaluation, we here demonstrated that Nrf2 KO mice have a fully preserved LV systolic function under baseline conditions, as indicated by unchanged CO, EF and SV, but accompanied by an increased MPI (also defined as Tei index [22]), which is an objective parameter representing both systolic and diastolic function [23]. These results indicated an impaired LV diastolic function in Nrf2 KO mice.

Diastolic dysfunction is mainly characterized by an impaired LV filling. Diastolic filling was evaluated here by a method considered as standard in the clinical routine, i.e. the transmitral inflow Doppler in apical four chamber view. The first hint of impaired myocardial relaxation in Nrf2 KO mice was a significantly prolonged DT and a prolonged IVRT. At the cellular level, IVRT represents the time, during which actin-myosin cross-bridges are returned to a low-force generation state, in a way that relaxation of the myocardium occurs and initiates diastolic filling of the ventricle [40]; therefore, IVRT is considered as the most sensitive Doppler index to detect an impaired cardiac relaxation [41]. Our results provide evidence that impaired myocardial relaxation is also correlated to a dysregulation of Ca^{2+} handling in the myocardium. It was shown that Nrf2-dependent signaling pathways play a role in the regulation of Ca^{2+} homeostasis in neurons [42]. Moreover, increased oxidative stress impairs Ca^{2+}-dependent signaling in the cardiomyocytes [35], and is involved in the dysregulation of ventricular remodeling. Evidence of Ca^{2+} dyshomeostasis in Nrf2 KO hearts was presented here. In addition to prolonged IVRT under baseline conditions in vivo, we found strongly decreased effects of isoproterenol and ouabain on myocardial relaxation. These drugs interfere with Ca^{2+} homeostasis in the cardiomyocytes, respectively inhibiting Ca^{2+} removal from the cytosol and inducing Ca^{2+} overload. Thus, in Nrf2 KO hearts the effects of isoproterenol on DP and dP/dt_{min} were lower than in WT mice. Moreover, we found no effects of ouabain application on dP/dt_{max} and dP/dt_{min} in Nrf2 KO mice, while in WT mice ouabain significantly increased both of those parameters. These results are consistent with decreased expressional levels of SERCA2a in the myocardium. SERCA2a is a major regulator of diastolic Ca^{2+} uptake in the sarcoplasmic reticulum and contribute to the regulation of Ca^{2+} homeostasis in cardiomyocytes [43]. If the expression/activity of SERCA2a is decreased in the cardiomyocytes, the Ca^{2+} removal into the sarcoplasmic reticulum is less efficient and results in an impaired relaxation during diastole as reflected by a decrease in IVRT in Nrf2 KO mice. In the clinical routine LV diastolic dysfunction is graded by severity as mild, pseudonormal, restrictive, and irreversible. In these mice we could not distinguish between pseudonormal and restrictive diastolic dysfunction. Cardiac diastolic dysfunction is mainly associated with an increase in the myocardial mass, as shown here by an increase in both, heart weight to body weight ratio and LV mass to body weight ratio. Decrease in LV relaxation can be correlated to the observed LV-hypertrophy, which leads to an increase in oxygen demand and a concomitant decrease in oxygen supply. These are associated with an increased stiffness of the cardiomyocytes and impairment in Ca^{2+} homeostasis.

Different studies suggest that pro-inflammatory cytokines like TNFα decrease the expression of SERCA2a in the myocardium [44]. We found neither changes in plasma TNFα levels in Nrf2 KO mice compared to WT littermates, nor any other signs of inflammatory phenotype in these mice. Nrf2 KO on ICR/SV129 background are known for showing a pro-inflammatory state from a certain age [32] and female mice develop an autoimmune-like disease [45]. The mice used in this study are Nrf2 KO on a C57Bl/6 background, they grow up normally and do not show any evidence of chronic inflammatory illness like increased leukocytes, edema, skin inflammation or strongly reduced body weight.

To summarize, the functional data obtained in vivo and in isolated working hearts demonstrate an impaired diastolic function associated with cardiac hypertrophy and decreased expression of SERCA2a in the myocardium of Nrf2 KO mice. Further studies should be conducted to analyze the mechanisms underpinning the dysregulation of Ca^{2+} homeostasis in the cardiomyocytes of Nrf2 KO mice.

4.2. Preserved endothelial function, hypotension and eNOS upregulation in Nrf2 KO mice

A growing body of evidence suggests that increased generation or decreased detoxification of radical oxygen species like superoxide radical anion ($O_2^{\bullet-}$), hydroxyl radicals and hydrogen peroxide lead to oxidative modification of target proteins, apoptosis, and tissue damage [46]. Many enzymatic sources of radical oxygen species such as membrane oxidase (like NADPH oxidases) or increased production of $O_2^{\bullet-}$ by the mitochondria have been implicated in vascular damage and increased vascular stiffness [46]. Likewise, decrease in NO bioavailability and endothelial dysfunction have been linked to eNOS dimer destabilization and enzyme uncoupling [46], leading to formation of $O_2^{\bullet-}$ and peroxynitrite as a result of the reaction of $O_2^{\bullet-}$ with NO. In vitro experiments have

demonstrated that NO-mediated Nrf2 activation plays a central role in protection of endothelial cells against oxidative damage [12,13]. Moreover it was shown that Nrf2-dependent regulation of gene expression is essential in keeping eNOS in the coupled state [34], as it regulates the synthesis of the cofactor tetrahydrobiopterin in HUVECs [34].

Therefore, in Nrf2 KO mice one would expect to find a dysfunctional eNOS, decreased NO bioavailability, endothelial dysfunction, increased vascular stiffness and hypertension. Instead, in Nrf2 KO mice we found significantly decreased blood pressure, fully preserved shear-stress-dependent flow-mediated vasodilation in vivo and aortic endothelium-dependent relaxation, as well as fully preserved pharmacological responses to bradykinin and carbachol in coronary and conduit vessels. Vascular stiffness was not increased, as demonstrated by lack of changes in pulse wave velocity. These physiological responses were fully blocked by the application of the specific NOS inhibitor ETU, which results in a significant increase in blood pressure and a loss of dilatory response after cuff release. Moreover, the basal cGMP levels in the aorta and in the heart, as well as the circulating nitrite and nitrate levels in Nrf2 KO mice are not significantly different from WT littermates, indicating a preserved NO bioavailability. On the other hand, both pharmacological inhibition of NOS in WT mice and genetic deletion of eNOS lead to a decrease in NO bioavailability [47], increase in blood pressure and vascular stiffness (assessed by PWV), as shown here and elsewhere [20,21]. Furthermore, aortic and myocardial eNOS phosphorylation level (Ser1177) were not changed in Nrf2 KO mice, suggesting that this post-translational modification is not involved in keeping endothelial function normal in these mice. These results are supported by a recent publication showing that eNOS preserves vascular function despite largely increases in vascular oxidative stress [48]. Taken together, results demonstrate that increased eNOS expression is a major underlying mechanism of preserved endothelial function and decreased blood pressure in Nrf2 KO mice.

Overexpression of eNOS in the heart and in the vessels of Nrf2 KO mice might be considered as a way to compensate detrimental changes in vascular tissues due to dysregulation of redox control and chronic adaptation to the lack of Nrf2. In Nrf2 KO mice the expression of antioxidant enzymes and enzymes responsible for the glutathione de novo synthesis are decreased of different extent in all tissues, including the heart and the vessels [3,16,32,49]. Accordingly, we observed a decrease in total GSH in the aorta and the heart of these mice, indicating decreased GSH-dependent antioxidant and detoxification capacity. Radical oxygen species (released by treatment with H_2O_2) have been shown to increase the eNOS expression and regulate its activity in vascular cells (e.g. via Ca^{2+} signaling) [50]. Therefore the molecular mechanisms linking the lack of Nrf2 to the increased eNOS expression in aorta and heart could be dependent on the decreased antioxidant and free radical detoxification capacity in Nrf2 KO mice, which may lead to accumulation of radical oxygen species (including superoxide anion radicals, hydroxyl radical and H_2O_2). Interestingly, an upregulation of eNOS expression was also found in atherosclerotic vessels [51]. In our model changes in eNOS expression are also accompanied by increase in expression of the NO-sensitive GC1 in the aorta, and a rightward shift of the NO-induced vasodilation of aortic rings, which may further contribute to maintenance of vascular function in Nrf2 KO mice. Although we cannot exclude that other compensatory redox-dependent mechanisms may contribute to maintenance of endothelial vascular function and to decreased blood pressure in mice lacking Nrf2, here we present compelling evidence showing that the eNOS-dependent patway plays a major role in compensating redox dysbalance, including increased eNOS/NO-GC1 expression and pharmacological activation of the pathway by carbachol, preserved endothelial-dependent vascular relaxation and NO bioavailability. Taken together, these data demonstrate that eNOS pathway play a central protective role in vascular protection in Nrf2 KO mice.

While the fundamental role played by eNOS activity in shear-stress dependent mechanotransduction and blood pressure regulation is well established [50], the role of eNOS in cardiac contraction, relaxation and heart rate is more complex (please refer to the excellent review by Balligand [50,52]). In the heart, eNOS is expressed both in the coronary endothelium and the cardiomyocytes [52]. NO endogenously produced in the heart by eNOS (and in part by the neuronal NOS) is thought to regulate changes in contractility in response to preload, as well as shear-dependent myocyte relaxation through cGMP-dependent desensitization of cardiac myofilaments [50]. At the same time, NO attenuates the positive inotropic effect of β-adrenergic stimulation and potentiates its lusitropic effect, which allows optimal adaptation of contraction-relaxation time intervals (favoring coronary perfusion) and recruitment of diastolic reserve [50]. This results into an equivalent of a “smart β-adrenergic blockade” [50], which is responsible for fine tuning and regulation of cardiac function [50].

A peculiarity of the shear-dependent vascular response in Nrf2 KO mice is the vasodilatory response occurring during cuff occlusion. On the contrary, a vasoconstrictory response was measured in WT mice (with or without NOS inhibition), as well as in eNOS KO mice. Similar findings were described in a comparable setting in humans [19]. The molecular mechanisms responsible for vasoconstriction of healthy vessels during occlusion (defined by Gori et al. as low-flow-mediated constriction) are not fully understood [19]. Based on pharmacological studies in humans, these authors proposed that low-flow mediated constriction is NOS-independent and might be mediated by a coordinated effect of an increased production of a vasoconstrictor (like endothelin 1) and the concomitant inhibition of a vasodilator, such as a cytochrome P450-derived endothelial hyperpolarizing factor (EDHF) and/or cyclooxygenase products (like prostaglandins). Our findings in WT mice treated with NOS inhibitor, as well as eNOS KO mice fully confirm that the low-flow vasoconstriction is NOS-independent. On the other hand, the paradoxical vasodilatory response during cuff-occlusion observed in Nfr2 KO mice may be due to changes in pathways involving those factors, or due to accumulation of vasodilators like H_2O_2 or $O_2^{\bullet -}$ [26,53], or rather may be a manifestation of altered Ca^{2+} handling in the vasculature (like observed in the Nrf2 KO heart) and/or a decreased response to vasoconstrictory stimuli of the vessels of these mice (as shown by a blunted PHE response of Nrf2 KO aortic rings). How exactly the lack of Nrf2 is involved in those changes, which enzymes are involved, and how overexpression of eNOS and NO production participate in these responses, these are all new aspects that should be specifically addressed in the future. The measurement of low-flow and high flow-dependent changes in rodents by applying the ultrasound method described in this paper, together with the observation that Nrf2 KO mice lack the vasoconstrictor responses under low flow conditions may allow a deeper understanding of this phenomena, which until now were only studied in humans.

Taken together, these results show that Nrf2 KO mice have a LV diastolic dysfunction, which is not related to changes in coronary vascular function and that eNOS upregulation contributes to preserve vascular endothelial function in these mice.

4.3. Summary, clinical significance and future directions

To summarize, we presented compelling evidence that mice lacking Nrf2 show a LV diastolic dysfunction characterized by a LV hypertrophy and downregulation of SERCA2a, by an impaired myocardial relaxation, and by an impaired Ca^{2+} handling in the heart. These changes are accompanied by a fully preserved

vascular function, decreased blood pressure and a compensatory increase in eNOS expression in the aorta and in the heart of these mice. Therefore, Nrf2-dependent pathways may be involved not only in cardiac remodeling [32] or changes in redox state of cardiac fibroblasts [15], but also in preserving cardiac function as shown here. Although LV diastolic dysfunction is a condition occurring in almost 50% of all patients affected by heart failure, and its prevalence rises by ~1% a year [54], the mechanisms responsible for this medical condition are not fully understood, and there is a lack of in vivo models of this disease. These results suggest that Nrf2 KO mice are a useful model for investigating the mechanisms underpinning the development of diastolic dysfunction, and put forward novel unexplored questions concerning the role of Nrf2-dependent biochemical pathways in pathophysiology of LV diastolic dysfunction and in vascular function, including (but not limited to) the control of Ca^{2+} homeostasis in cardiomyocytes (as described for neurons before [42]), the regulation of vessel tone during low flow mediated vasoconstriction, and Nrf2-related regulation of eNOS expression and nitric oxide bioavailability in the cardiovascular system.

Author contributions

M.M.C.-K. conceived and initiated the study; R.E., M.K., M.M.C.-K. designed research; R.E., M.K., M.M.C.-K. wrote the paper; R.E., C. M.K., W.L., T.S., M.M.C.-K. contributed to manuscript draft and concept; R.E., C.M.K., W.L., C.P., L.K., T.K., M.W., J.D., E.M, T.S., M.M. C.-K performed research and contributed to data analysis and statistics.

The authors declare no conflict of interest

None

Acknowledgments

We wish to thank Stefanie Becher for expert technical assistance, and Dr. rer. nat. Simone Gorressen for helping with the echocardiographic analysis. Furthermore we are grateful to the German Research Council (DFG CO 1305/2-1 to M.M.C.-K., SFB1116 TP B06 to M.M.C.-K. and M.K.), to the Forschungskommission of the Universitätsklinikum Düsseldorf (to M.M.C.K.) and the Susanne-Bunnenberg-Stiftung of the Düsseldorf Heart Center (to M. K.), for financial support.

Appendix A. Supplementary material

Supplementary data associated with this article can be found in the online version at http://dx.doi.org/10.1016/j.freeradbiomed.2015.10.409.

References

[1] T. Suzuki, M. Yamamoto, Molecular basis of the Keap1-Nrf2 system, Free Radic. Biol. Med. (2015).
[2] K. Itoh, T. Chiba, S. Takahashi, T. Ishii, K. Igarashi, Y. Katoh, T. Oyake, N. Hayashi, K. Satoh, I. Hatayama, M. Yamamoto, Y. Nabeshima, An Nrf2/small Maf heterodimer mediates the induction of phase II detoxifying enzyme genes through antioxidant response elements, Biochem. Biophys. Res. Commun. 236 (1997) 313–322.
[3] A. Enomoto, K. Itoh, E. Nagayoshi, J. Haruta, T. Kimura, T. O'Connor, T. Harada, M. Yamamoto, High sensitivity of Nrf2 knockout mice to acetaminophen hepatotoxicity associated with decreased expression of ARE-regulated drug metabolizing enzymes and antioxidant genes, Tox. Sci 59 (2001) 169–177.
[4] H. Sies, Oxidative stress: a concept in redox biology and medicine, Redox biol (2015).
[5] M. Seddon, Y.H. Looi, A.M. Shah, Oxidative stress and redox signalling in cardiac hypertrophy and heart failure, Heart 93 (2007) 903–907.
[6] E. Kansanen, S.M. Kuosmanen, H. Leinonen, A.-L. Levonen, The Keap1-Nrf2 pathway: Mechanisms of activation and dysregulation in cancer, Redox biol 1 (2013) 45–49.
[7] L. Gan, J.A. Johnson, Oxidative damage and the Nrf2-ARE pathway in neurodegenerative diseases, Biochim. Biophys. Acta 1842 (2014) 1208–1218.
[8] J. Pi, L. Leung, P. Xue, W. Wang, Y. Hou, D. Liu, E. Yehuda-Shnaidman, C. Lee, J. Lau, T.W. Kurtz, J.Y. Chan, Deficiency in the nuclear factor E2-related factor-2 transcription factor results in impaired adipogenesis and protects against diet-induced obesity, J. Biol. Chem. 285 (2010) 9292–9300.
[9] A. Alfieri, S. Srivastava, R.C. Siow, M. Modo, P.A. Fraser, G.E. Mann, Targeting the Nrf2–Keap1 antioxidant defence pathway for neurovascular protection in stroke, J. Physiol. 589 (2011) 4125–4136.
[10] A. Uruno, Y. Yagishita, M. Yamamoto, The Keap1–Nrf2 system and diabetes mellitus, Arch. Biochem. Biophys. 566 (2015) 76–84.
[11] H. Zhang, K.J. Davies, H.J. Forman, Oxidative stress response and Nrf2 signaling in aging, Free Radic. Biol. Med. (2015).
[12] M.M. Cortese-Krott, C.V. Suschek, W. Wetzel, K.-D. Kröncke, V. Kolb-Bachofen, Nitric oxide-mediated protection of endothelial cells from hydrogen peroxide is mediated by intracellular zinc and glutathione, Am. J. Physiol.- Cell. Ph 296 (2009) C811–C820.
[13] M.M. Cortese, C.V. Suschek, W. Wetzel, K.-D. Kröncke, V. Kolb-Bachofen, Zinc protects endothelial cells from hydrogen peroxide via Nrf2-dependent stimulation of glutathione biosynthesis, Free Radic. Biol. Med. 44 (2008) 2002–2012.
[14] H. Zhu, Z. Jia, B.R. Misra, L. Zhang, Z. Cao, M. Yamamoto, M.A. Trush, H.P. Misra, Y. Li, Nuclear factor E2-related factor 2-dependent myocardiac cytoprotection against oxidative and electrophilic stress, Cardiovasc. Toxicol. 8 (2008) 71–85.
[15] A.C. Brewer, T.V. Murray, M. Arno, M. Zhang, N.P. Anilkumar, G.E. Mann, A. M. Shah, Nox4 regulates Nrf2 and glutathione redox in cardiomyocytes in vivo, Free Radic. Biol. Med. 51 (2011) 205–215.
[16] J.W. Calvert, S. Jha, S. Gundewar, J.W. Elrod, A. Ramachandran, C.B. Pattillo, C. G. Kevil, D.J. Lefer, Hydrogen sulfide mediates cardioprotection through Nrf2 signaling, Circ. Res. 105 (2009) 365–374.
[17] B. Xu, J. Zhang, J. Strom, S. Lee, Q.M. Chen, Myocardial ischemic reperfusion induces de novo Nrf2 protein translation, Biochim. Biophys. Acta 1842 (2014) 1638–1647.
[18] M. Kelm, Flow-mediated dilatation in human circulation: diagnostic and therapeutic aspects, Am. J. Physiol: Heart and Circ. Physiol 282 (2002) H1–H5.
[19] T. Gori, S. Dragoni, M. Lisi, G. Di Stolfo, S. Sonnati, M. Fineschi, J.D. Parker, Conduit artery constriction mediated by low flow a novel noninvasive method for the assessment of vascular function, J. Am. Coll. Cardiol. 51 (2008) 1953–1958.
[20] A. Gödecke, U.K. Decking, Z. Ding, J. Hirchenhain, H.-J. Bidmon, S. Gödecke, J. Schrader, Coronary hemodynamics in endothelial NO synthase knockout mice, Circ. Res. 82 (1998) 186–194.
[21] K.C. Wood, M.M. Cortese-Krott, J.C. Kovacic, A. Noguchi, V.B. Liu, X. Wang, N. Raghavachari, M. Boehm, G.J. Kato, M. Kelm, Circulating blood endothelial nitric oxide synthase contributes to the regulation of systemic blood pressure and nitrite homeostasis, Arterioscler. Thromb. Vasc. Biol. 33 (2013) 1861–1871.
[22] C. Tei, R.A. Nishimura, J.B. Seward, A.J. Tajik, Noninvasive Doppler-derived myocardial performance index: correlation with simultaneous measurements of cardiac catheterization measurements, J. Am. Soc. Echocard 10 (1997) 169–178.
[23] J. Ärnlöv, E. Ingelsson, U. Risérus, B. Andrén, L. Lind, Myocardial performance index, a Doppler-derived index of global left ventricular function, predicts congestive heart failure in elderly men, Eur. Heart J. 25 (2004) 2220–2225.
[24] D. Schuler, R. Sansone, T. Freudenberger, A. Rodriguez-Mateos, G. Weber, T. Y. Momma, C. Goy, J. Altschmied, J. Haendeler, J.W. Fischer, M. Kelm, C. Heiss, Measurement of endothelium-dependent vasodilation in mice—Brief Report, Arterioscler. Thromb. Vasc. Biol. 34 (2014) 2651–2657.
[25] C. Rammos, U.B. Hendgen-Cotta, R. Deenen, J. Pohl, P. Stock, C. Hinzmann, M. Kelm, T. Rassaf, Age-related vascular gene expression profiling in mice, Mech. Ageing Dev. 135 (2014) 15–23.
[26] T. Suvorava, N. Lauer, S. Kumpf, R. Jacob, W. Meyer, G. Kojda, Endogenous vascular hydrogen peroxide regulates arteriolar tension in vivo, Circulation 112 (2005) 2487–2495.
[27] U. Flögel, U.K. Decking, A. Gödecke, J. Schrader, Contribution of NO to ischemia-reperfusion injury in the saline-perfused heart: a study in endothelial NO synthase knockout mice, J. Mol. Cell. Cardiol. 31 (1999) 827–836.
[28] P. Pacher, T. Nagayama, P. Mukhopadhyay, S. Bátkai, D.A. Kass, Measurement of cardiac function using pressure–volume conductance catheter technique in mice and rats, Nat. Protoc. 3 (2008) 1422–1434.
[29] E. Mergia, A. Friebe, O. Dangel, M. Russwurm, D. Koesling, Spare guanylyl cyclase NO receptors ensure high NO sensitivity in the vascular system, J. Clin. Invest. 116 (2006) 1731–1737.
[30] T. Rassaf, N.S. Bryan, M. Kelm, M. Feelisch, Concomitant presence of N-nitroso and S-nitroso proteins in human plasma, Free Radic. Biol. Med. 33 (2002) 1590–1596.
[31] X. He, Q. Ma, Redox regulation by nuclear factor erythroid 2-related factor 2: gatekeeping for the basal and diabetes-induced expression of thioredoxin-interacting protein, Mol. Pharmacol. 82 (2012) 887–897.

[32] J. Li, T. Ichikawa, L. Villacorta, J.S. Janicki, G.L. Brower, M. Yamamoto, T. Cui, Nrf2 protects against maladaptive cardiac responses to hemodynamic stress, Arterioscler. Thromb. Vasc. Biol. 29 (2009) 1843–1850.
[33] Lacher, S.E.; Lee, J.S.; Wang, X.; Campbell, M.R.; Bell, D.A.; Slattery, M. Beyond antioxidant genes in the ancient Nrf2 regulatory network. *Free Radical Biol. Med*.
[34] E.H. Heiss, D. Schachner, E.R. Werner, V.M. Dirsch, Active NF-E2-related factor (Nrf2) contributes to keep endothelial NO synthase (eNOS) in the coupled state role of reactive oxygen species (ROS), eNOS, and heme oxygenase (HO-1) levels, J. Biol. Chem. 284 (2009) 31579–31586.
[35] C.X. Santos, N. Anilkumar, M. Zhang, A.C. Brewer, A.M. Shah, Redox signaling in cardiac myocytes, Free Radic. Biol. Med. 50 (2011) 777–793.
[36] Y. Ding, B. Zhang, K. Zhou, M. Chen, M. Wang, Y. Jia, Y. Song, Y. Li, A. Wen, Dietary ellagic acid improves oxidant-induced endothelial dysfunction and atherosclerosis: role of Nrf2 activation, Int. J. Cardiol. 175 (2014) 508–514.
[37] M. Buelna-Chontal, J.-G. Guevara-Chávez, A. Silva-Palacios, O.-N. Medina-Campos, J. Pedraza-Chaverri, C. Zazueta, Nrf2-regulated antioxidant response is activated by protein kinase C in postconditioned rat hearts, Free Rad. Biol. Med 74 (2014) 145–156.
[38] H. Tsutsui, S. Kinugawa, S. Matsushima, Oxidative stress and heart failure, Am. J. Physiol. Heart Circ. Physiol 301 (2011) H2181–H2190.
[39] L. Cominacini, C. Mozzini, U. Garbin, A. Pasini, C. Stranieri, E. Solani, P. Vallerio, I.A. Tinelli, A. Fratta Pasini, Endoplasmic reticulum stress and Nrf2 signaling in cardiovascular diseases, Free Radic. Biol. Med. (2015).
[40] P. Giannuzzi, A. Imparato, P.L. Temporelli, F. de Vito, P.L. Silva, F. Scapellato, A. Giordano, Doppler-derived mitral deceleration time of early filling as a strong predictor of pulmonary capillary wedge pressure in postinfarction patients with left ventricular systolic dysfunction, J. Am. Coll. Cardiol. 23 (1994) 1630–1637.
[41] M.J. García, L. Rodríguez, M. Ares, B.P. Griffin, J.D. Thomas, A.L. Klein, Differentiation of constrictive pericarditis from restrictive cardiomyopathy: assessment of left ventricular diastolic velocities in longitudinal axis by Doppler tissue imaging, J. Am. Coll. Cardiol. 27 (1996) 108–114.
[42] J.-M. Lee, A.Y. Shih, T.H. Murphy, J.A. Johnson, NF-E2-related factor-2 mediates neuroprotection against mitochondrial complex I inhibitors and increased concentrations of intracellular calcium in primary cortical neurons, J. Biol. Chem. 278 (2003) 37948–37956.
[43] M.A. Shareef, L.A. Anwer, C. Poizat, Cardiac SERCA2a/b: therapeutic targets for heart failure, Eur J. Pharmacol. 724 (2014) 1–8.
[44] C.T. Tsai, C.K. Wu, J.K. Lee, S.N. Chang, Y.M. Kuo, Y.C. Wang, L.P. Lai, F.T. Chiang, J.J. Hwang, J.L. Lin, TNF-alpha down-regulates sarcoplasmic reticulum Ca(2)(+) ATPase expression and leads to left ventricular diastolic dysfunction through binding of NF-kappaB to promoter response element, Cardiovasc. Res. 105 (2015) 318–329.
[45] K. Yoh, K. Itoh, A. Enomoto, A. Hirayama, N. Yamaguchi, M. Kobayashi, N. Morito, A. Koyama, M. Yamamoto, S. Takahashi, Nrf2-deficient female mice develop lupus-like autoimmune nephritis, Kidney Int. 60 (2001) 1343–1353.
[46] H. Li, S. Horke, U. Forstermann, Vascular oxidative stress, nitric oxide and atherosclerosis, Atherosclerosis 237 (2014) 208–219.
[47] P. Kleinbongard, A. Dejam, T. Lauer, T. Jax, S. Kerber, P. Gharini, J. Balzer, R. B. Zotz, R.E. Scharf, R. Willers, A.N. Schechter, M. Feelisch, M. Kelm, Plasma nitrite concentrations reflect the degree of endothelial dysfunction in humans, Free Radic. Biol. Med. 40 (2006) 295–302.
[48] T. Suvorava, N. Nagy, S. Pick, O. Lieven, U. Ruther, V.T. Dao, J.W. Fischer, M. Weber, G. Kojda, Impact of eNOS-Dependent Oxidative Stress on Endothelial Function and Neointima Formation, Antioxid. Redox Signal. 23 (2015) 711–723.
[49] H.K. Jyrkkanen, E. Kansanen, M. Inkala, A.M. Kivela, H. Hurttila, S.E. Heinonen, G. Goldsteins, S. Jauhiainen, S. Tiainen, H. Makkonen, O. Oskolkova, T. Afonyushkin, J. Koistinaho, M. Yamamoto, V.N. Bochkov, S. Yla-Herttuala, A. L. Levonen, Nrf2 regulates antioxidant gene expression evoked by oxidized phospholipids in endothelial cells and murine arteries in vivo, Circ. Res. 103 (2008), e1-9.
[50] J.-L. Balligand, O. Feron, C. Dessy, eNOS activation by physical forces: from short-term regulation of contraction to chronic remodeling of cardiovascular tissues, Physiol. Rev. 89 (2009) 481–534.
[51] J.B. Laursen, M. Somers, S. Kurz, L. McCann, A. Warnholtz, B.A. Freeman, M. Tarpey, T. Fukai, D.G. Harrison, Endothelial regulation of vasomotion in apoE-deficient mice: implications for interactions between peroxynitrite and tetrahydrobiopterin, Circulation 103 (2001) 1282–1288.
[52] P. Massion, J.-L. Balligand, Modulation of cardiac contraction, relaxation and rate by the endothelial nitric oxide synthase (eNOS): lessons from genetically modified mice, J. Physiol. 546 (2003) 63–75.
[53] T. Suvorava, G. Kojda, Reactive oxygen species as cardiovascular mediators: lessons from endothelial-specific protein overexpression mouse models, Biochim. Biophys. Acta 1787 (2009) 802–810.
[54] T.E. Owan, D.O. Hodge, R.M. Herges, S.J. Jacobsen, V.L. Roger, M.M. Redfield, Trends in prevalence and outcome of heart failure with preserved ejection fraction, N. Engl. J. Med. 355 (2006) 251–259.